ELSEVIER

Journal of Hazardous Materials B138 (2006) 304–310

Journal of Hazardous Materials

www.elsevier.com/locate/jhazmat

Adsorption thermodynamic and kinetic studies of trihalomethanes on multiwalled carbon nanotubes

Chungsying Lu *, Yao-Lei Chung, Kuan-Foo Chang

Department of Environmental Engineering, National Chung Hsing University, 250 Kuo Kuang Road, Taichung 402, Taiwan

Received 31 March 2005; received in revised form 22 August 2005; accepted 1 May 2006
Available online 2 June 2006

Abstract

Multiwalled carbon nanotubes (MWCNTs) were purified by mixed HNO_3/H_2SO_4 solution and were employed as adsorbents to study adsorption kinetics and thermodynamics of trihalomethanes (THMs) from chlorinated drinking water. The amount of THMs adsorbed onto CNTs decreased with a rise in temperature and high adsorption capacities were found at 5 and 15 °C. Under the same conditions, the purified CNTs possess two to three times more adsorption capacities of $CHCl_3$, which accounts for a major portion of THMs in the chlorinated drinking water, than the commercially available PAC suggesting that CNTs are efficient adsorbents. The thermodynamic analysis revealed that the adsorption of THMs onto CNTs is exothermic and spontaneous.

Keywords: Carbon nanotubes; Adsorption; Trihalomethanes; Kinetics; Thermodynamics

1. Introduction

Disinfection is routinely carried out in water treatment process or before finished water leaves the treatment plant to prevent microbiological degradation of drinking water quality [1]. Until recently chlorine is still the most commonly employed disinfectant and minimum chlorine residues must be maintained to ensure the disinfection capacity of drinking water [2]. However, disinfection by-products (DBPs) such as trihalomethanes (THMs; $CHCl_3$, $CHBrCl_2$, $CHBr_2Cl$, and $CHBr_3$) were found to be formed during the chlorination of drinking water [3]. THMs are recognized as potentially hazardous and carcinogenic substances [4]. Therefore, more stringent requirements for the removal of THMs from drinking water necessitate the development of innovative, cost effective treatment alternatives.

Carbon nanotubes (CNTs) are unique and one-dimensional macromolecules that possess outstanding thermal and chemical stability [5]. These nanomaterials have been proven to possess great potential as adsorbents for removing many kinds of environmental pollutants. Long and Yang [6] reported that a significantly higher dioxin removal efficient is found with CNTs than that with activated carbon. Li et al. [7] indicated that CNTs have high lead adsorption capacity and can be used as an adsorbent for lead removal from water. Li et al. [8] showed that CNTs are good fluoride adsorbents and their fluoride removal capability is superior to activated carbon. Peng et al. [9] found that CNTs are good adsorbents to remove 1, 2-dichlorobenzene from water and can be used in a wide pH range 3–10. Recently, we have demonstrated that both NaClO oxidized single-walled CNTs (SWCNTs) and multi-walled CNTs (MWCNTs) are effective Zn^{2+} sorbents [10] and can be reused through 10 cycles of water treatment and regeneration [11].

This paper investigated the effect of temperature change in the range 5–35 °C (in 10 °C increments) on the adsorption of THMs from chlorinated drinking water by HNO_3/H_2SO_4 purified MWCNTs. The kinetic and thermodynamic parameters of adsorption process were also calculated and analyzed.

2. Materials and methods

2.1. Adsorbent

MWCNTs with outer diameter range 10–30 nm and inner diameter range 5–10 nm (Model CN3016, Nanotech Port Co., Shenzhen, China) were selected as adsorbents in this study. The MWCNTs were fabricated by catalytic decomposition of the

* Corresponding author. Tel.: +886 4 22852483; fax: +886 4 22862587.
E-mail address: clu@nchu.edu.tw (C. Lu).

0304-3894/$ – see front matter © 2006 Elsevier B.V. All rights reserved.
doi:10.1016/j.jhazmat.2006.05.076

CH_4/H_2 mixture at 700 °C using Ni nanoparticles as catalyst. The length of CNTs was in the range 0.5–500 μm and the amorphous carbon content in the CNTs was less than 5%. These data were provided by the manufacturer.

One gram of raw CNTs was dispersed into a 150 ml flask containing 40 ml mixed acid solutions (30 ml of HNO_3 + 10 ml of H_2SO_4) for 24 h to remove metal catalysts (Ni nanoparticles) and then washed by deionized water. After cleaning, the CNTs were again dispersed into a 150 ml flask containing 40 ml of mixed acid solutions, which were then shaken in an ultrasonic cleaning bath (Branson 3510 Ultrasonic Cleaner, Connecticut, USA) and heated at 80 °C in water bath for 2 h to remove amorphous carbon. After cooling to room temperature, the mixture was filtered with a 0.45 μm glass-fiber filter and the solid was washed with deionized water until the pH of the filtrate was 7. The filtered solid was then dried at 80 °C for 2 h to give ∼0.967 g of purified CNTs.

2.2. Adsorbate

THMs solution was prepared by diluting a 2000 mg l^{-1} analytical grade THMs solution (Supelco Inc., Bellefonte, PA, USA), which contains equivalent concentration of $CHCl_3$, $CHCl_2Br$, $CHClBr_2$ and $CHBr_3$, into deionized water to obtain the desired THMs concentration.

2.3. Batch adsorption experiments

Batch adsorption experiments were conducted using 150 ml glass bottles with addition of 50 mg of purified CNTs and 125 ml of THMs solution of initial concentrations (C_0) from 0.2 to 12 mg l^{-1}. The glass bottles were sealed with 20 mm rubber stopper and then were mounted on a shaker, which was operated at 200 rpm for 24 h. The experiments were carried out at 5, 15, 25 and 35 °C in a temperature control box (Model CH-502, Chin Hsin, Taipei, Taiwan). The choice of agitation speed of 200 rpm is to provide a high degree of mixing. The choice of temperature range is to simulate possible water temperature in the field. The initial pH of the solution was adjusted at neutrality using 1 M H_2SO_4 or 1 M NaOH.

The amount of adsorbed THMs were calculated as follows:

$$q = (C_o - C_t)\frac{V}{m} \quad (1)$$

where q is the amount of adsorbed THM molecules onto CNTs (mg g^{-1}), C_0 the initial THMs concentration (mg l^{-1}), C_t the THMs concentration after a certain period of time (mg l^{-1}), V the initial solution volume (l) and m is the weight of CNTs (g).

2.4. Analytical methods

THMs concentration was determined using a gas chromatograph (Hewlett Packard Model 5890 II gas chromatograph, MD, USA) equipped with a electron capture detector (ECD). A 30 m HP-5 fused silica capillary column (0.25 mm inside diameter, 1.5 μm film thickness) was used for THMs analysis. The GC-ECD was operated at injection temperature of 177 °C, detector temperature of 272 °C and oven temperature of 110 °C. The morphology of CNTs was analyzed by a field emission scanning electron microscope (FE-SEM, JEOL JSM-6700, Tokyo, Japan) and a high-resolution transmission electron microscope (HR-TEM, JEOL JEM-2010, Tokyo, Japan). Surface area and pore size distribution (including average pore diameter and pore volume) of purified CNTs were calculated from nitrogen adsorption and desorption isotherm data measured by a BET sorptometer (Model BET-202A, Porous Materials Inc., New York, USA). The carbon content in the CNTs was analyzed by a thermogravimetric analyzer (Model Labsys TG-DSC 131, Setaram Instrumentation, Galuire, France). The functional groups on the surface of CNTs were detected by a Fourier transform infrared (FT-IR) spectroscopy (Model FT/IR-200, JAS Co., Tokyo, Japan).

3. Results and discussion

3.1. Characterization of purified CNTs

Fig. 1 shows the SEM image of purified CNTs. It is seen that the isolated MWCNTs usually curve and have cylindrical shapes with an external diameter of ∼25 nm. Due to inter-molecular force, the isolated CNTs of different size and direction form an aggregated structure. Fig. 2 displays the TEM image of a purified CNT. As can be observed, the purified CNT has a multiple atomic layers structure with the hollow inner tube diameter of ∼8 nm.

Pore size of purified CNTs can be characterized as a bimodal distribution including a fine fraction and a coarse fraction. The pores in the coarse fraction are likely to be contributed by aggregated pores which are formed with within the confined space among the isolated CNTs. The pores in the fine fraction are the CNT inner cavities, close to the inner CNT diameter. The fine and coarse fractions of purified CNTs were concentrated in the 2–8 and 40–80 nm width range, respectively. The inner and aggregated pores of CNTs are responsible for ∼50% and 20% of the total pore volume. The rest 30% of the total pore volume are in the pore size range 8–40 and 80–200 nm. Surface area of CNTs increased from 225 to 295 $m^2\ g^{-1}$ after acid treatment.

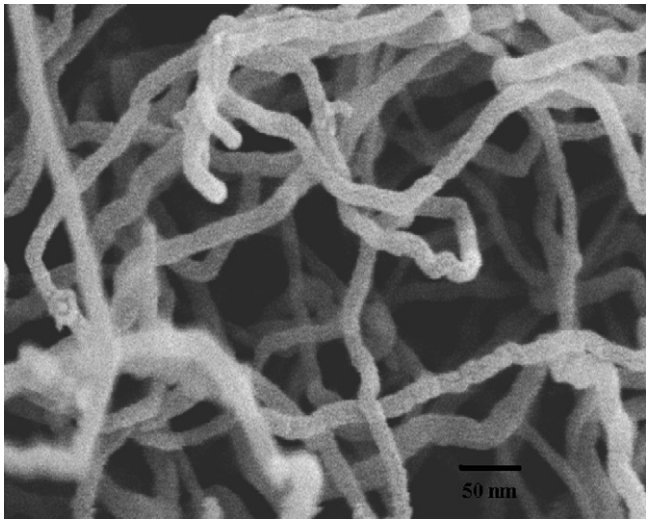

Fig. 1. Scanning electron microscope (SEM) image of purified CNTs.

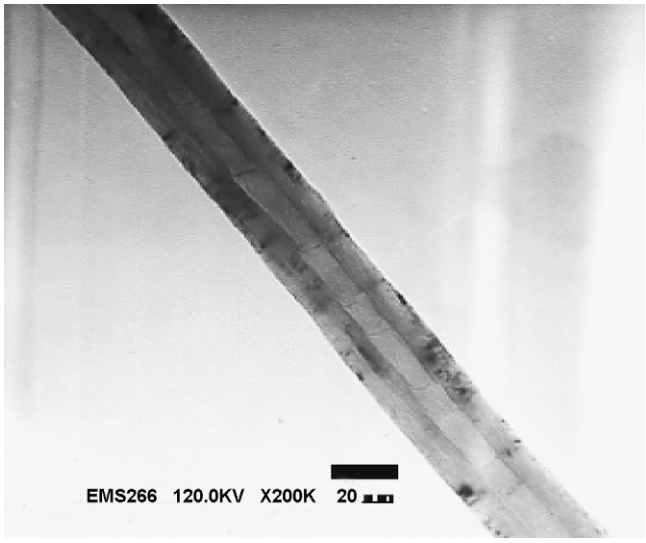

Fig. 2. Transmission electron microscope (TEM) image of purified CNTs.

Possible reason may be attributed to the fact that the acid treatment can untie entwined CNTs and thus increase the surface area of CNTs.

Thermogravimetric analysis revealed that purified CNTs are considerably stable and show a little weight loss close to 5% below 600 °C. A significant gasification begins at 600 °C and ends at ~700 °C, in which 1.13% remaining weight was found, indicating particularly high carbon content in the purified CNTs (98.87%).

The IR spectrum of purified CNTs exhibited three major peaks at ~1400, 1700 and 3500 cm^{-1}, which are associated with carboxylic acids and phenolic groups (O–H), carbonyl groups (>C=O) and hydroxyl groups (−OH), respectively [12]. These oxygen-containing functional groups produced abundantly on the external and internal surface of CNT pores, which can provide numerous chemical adsorption sites and thus increase the adsorption capacity for THM molecules. Many other functional groups attached on the surface of purified CNTs were also observed.

3.2. Effects of contact time and temperature

Figs. 3–6 show the effect of temperature on the adsorption rate of $CHCl_3$, $CHBrCl_2$, $CHBr_2Cl$ and $CHBr_3$ by CNTs, respectively, with a C_0 of 1.6 mg l^{-1}. For all the experiments, the amount of THM molecules adsorbed onto CNTs (q) increased quickly with time and then slowly reached equilibrium. With the exception for adsorption of $CHBr_3$ at 25 °C, the adsorption reached equilibrium at 150 min without regard to temperature. The amounts of THM molecules adsorbed onto CNTs at equilibrium (q_e) at 5, 15, 25 and 35 °C, respectively, are 0.87, 0.85, 0.82 and 0.72 mg g^{-1} for the $CHCl_3$; 0.52, 0.51, 0.47 and 0.39 mg g^{-1} for the $CHBrCl_2$; 0.55, 0.50, 0.44 and 0.38 mg g^{-1} for the $CHBr_2Cl$; 0.43, 0.42, 0.39 and 0.34 mg g^{-1} for the $CHBr_3$. The q_e value of $CHCl_3$ is the greatest, followed by $CHBrCl_2$, $CHBr_2Cl$ and then $CHBr_3$. This may be attributed to the oxygen-containing groups attached on the surface of purified

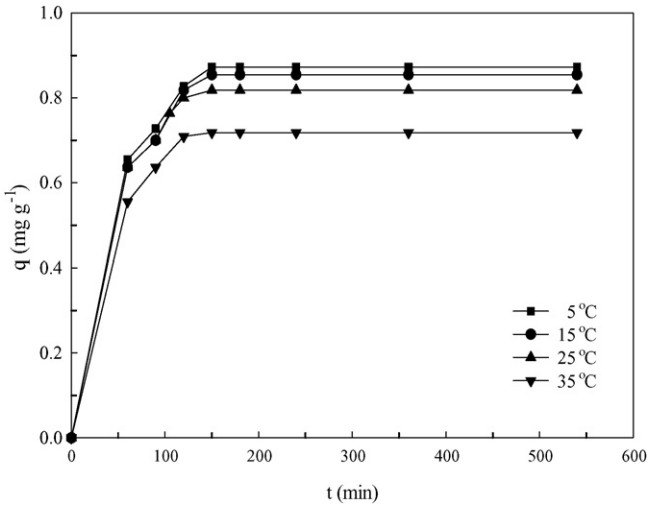

Fig. 3. Effect of temperature on the adsorption rate of $CHCl_3$ by CNTs.

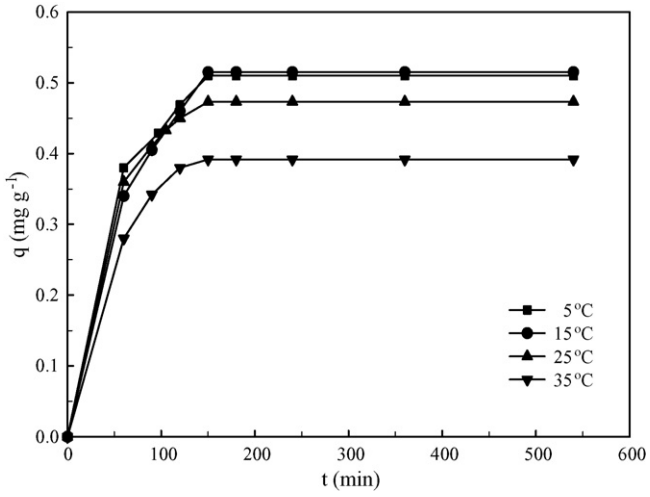

Fig. 4. Effect of temperature on the adsorption rate of $CHBrCl_2$ by CNTs.

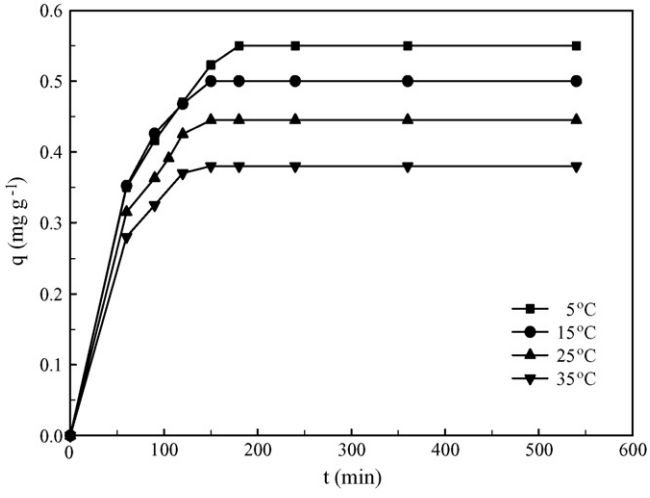

Fig. 5. Effect of temperature on the adsorption rate of $CHBr_2Cl$ by CNTs.

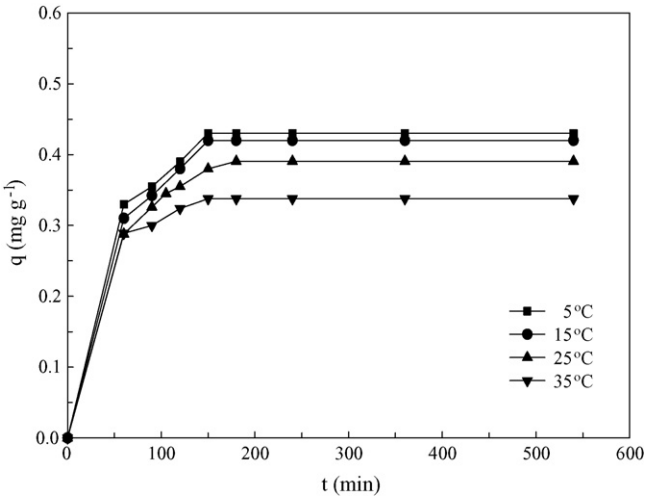

Fig. 6. Effect of temperature on the adsorption rate of $CHBr_3$ by CNTs.

CNTs, which made CNTs become more hydrophilic and suitable for adsorption of low molecular-weight THM molecules.

3.3. Kinetics of adsorption

To analyze the adsorption rate of THMs onto CNTs, the Lagergren's first-order rate equation is employed [13]:

$$\ln\frac{q_e - q_t}{q_e} = -k_1 t \quad (2)$$

where q_t are the amount of THMs adsorbed onto CNTs at time t (mg g^{-1}) and k_1 is the first-order rate constant (min^{-1}). The k_1 values under various temperatures can be determined by the slope of a linear plot of $\ln[(q_e - q_t)/q_e]$ versus t and are given in Table 1. The correlation coefficients (r^2) are all >0.96 indicating that the kinetics of THMs adsorption by CNTs follows the first-order rate law. The k_1 value increased with a rise in temperature, which could be explained by the fact that increasing temperature results in a rise in diffusion rate of THM molecules across the external boundary layer and within the pores of CNTs due to the result of decreasing solution viscosity. However, the temperature dependence of the k_1 value is inconsistent with the temperature dependence of the q_e value. This may be explained by the fact that adsorption rate is faster than desorption rate at a low temperature but desorption rate is more sensitive to temperature and it becomes greater at a high temperature. Therefore, adsorption would dominate at lower temperatures while desorption would dominate at higher temperatures [14].

Table 1
Rate constants of THMs adsorption by CNTs

THM molecules	k_1 (min^{-1})			
	5 °C	15 °C	25 °C	35 °C
$CHCl_3$	0.0284	0.0328	0.0357	0.0415
$CHBrCl_2$	0.0186	0.0193	0.0259	0.0375
$CHBr_2Cl$	0.0217	0.0255	0.0291	0.0384
$CHBr_3$	0.0153	0.0169	0.0179	0.0211

The temperature effect on the rate constant has been found in practically all cases to be well represented by the Arrhenius equation,

$$\ln k_1 = \ln A - \frac{E_a}{RT} \quad (3)$$

where A is the frequency of adsorption (min^{-1}), E_a the activation energy of the reaction (J mol^{-1}), R the universal gas constant (8.314 J mol^{-1} K^{-1}), and T is the absolute temperature. For all four THM molecules, a plot of $\ln k_1$ against the reciprocal of absolute temperature, $1/T$, gives a straight line, and the corresponding A and E_a are determined from the intercept and the slope, respectively, of each regression line. The r^2 values are all >0.96. The A values of $CHCl_3$, $CHBrCl_2$, $CHBr_2Cl$ and $CHBr_3$, respectively, are 4.08, 2.33, 1.68 and 0.42 min^{-1}. The A value is temperature-independent and becomes small for adsorption of large molecular-weight TMH molecules. The E_a values of $CHCl_3$, $CHBrCl_2$, $CHBr_2Cl$ and $CHBr_3$, respectively, are 8.85, 16.86, 13.06 and 9.68 kJ mol^{-1}. These values were small (<20 kJ mol^{-1}) showing that adsorption of THMs onto CNTs is controlled by diffusion mechanism [15].

3.4. Adsorption isotherms

Figs. 7–10 show the adsorption isotherms of $CHCl_3$, $CHBrCl_2$, $CHBr_2Cl$ and $CHBr_3$, respectively, by CNTs at various temperatures. It is apparent that the q_e value increased with a decrease in temperature and high q_e values were found at 5 and 15 °C. The adsorption isotherm curves at 5 and 15 °C are relatively close reflecting that the effects of temperature change on the THMs adsorption by CNTs are less significant from 5 to 15 °C than from 15 to 45 °C.

With a C_e of 1 mg l^{-1}, the q_e value of $CHCl_3$ by CNTs is 2.42 mg g^{-1}, which is more than those of 2.15 mg g^{-1} by carbon sphere reported in the literature [16] and of 1.2 mg g^{-1} by the commercially available PAC (San Ying Enterprises Co., Taipei, Taiwan) measured at 25 °C in this study. Although the BET surface area of CNTs (295 m^2 g^{-1}) is much less than those of carbon

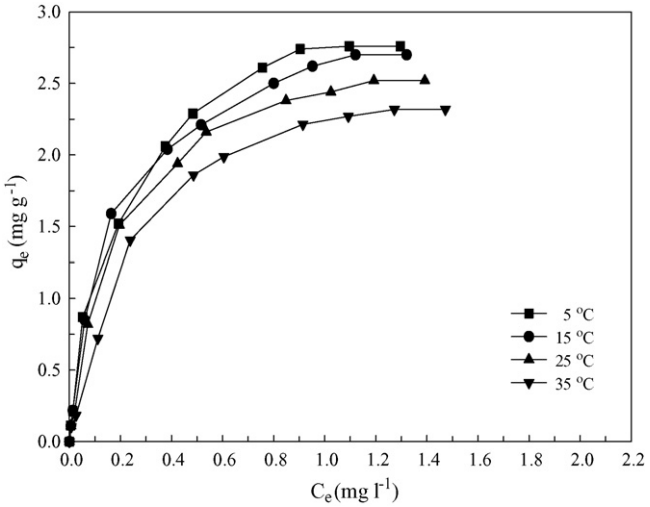

Fig. 7. Adsorption isotherms of $CHCl_3$ by CNTs at various temperatures.

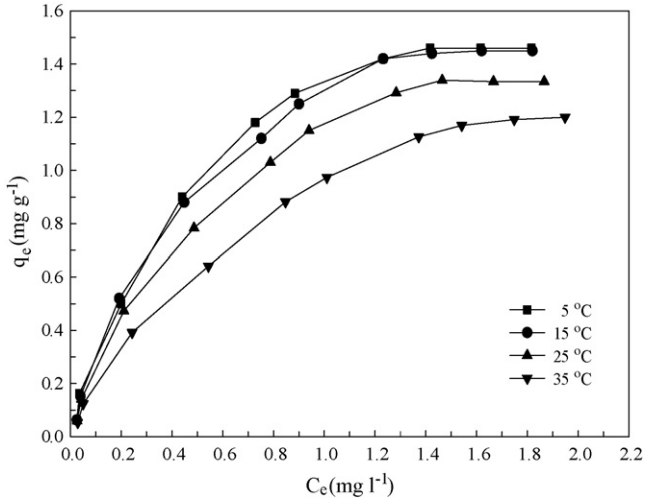

Fig. 8. Adsorption isotherms of $CHBrCl_2$ by CNTs at various temperatures.

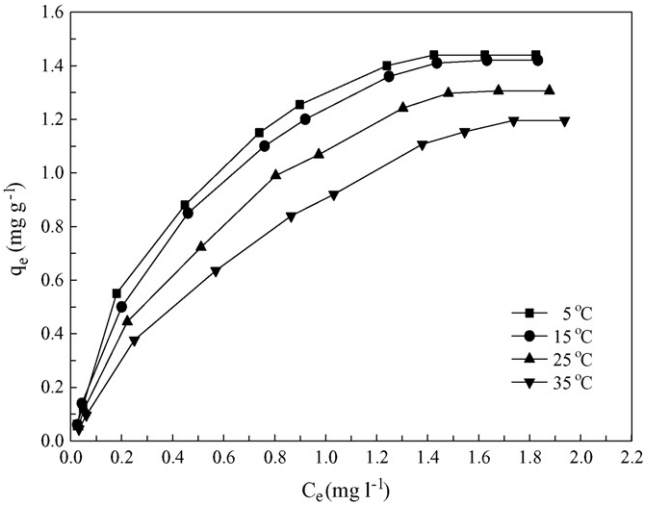

Fig. 9. Adsorption isotherms of $CHBr_2Cl$ by CNTs at various temperatures.

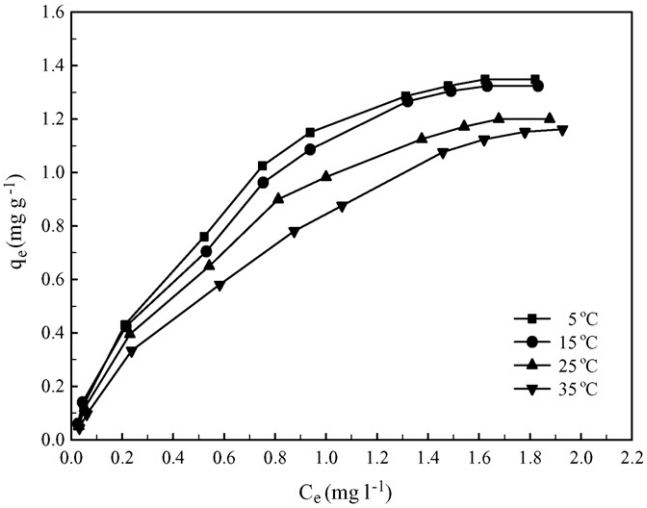

Fig. 10. Adsorption isotherms of $CHBr_3$ by CNTs at various temperatures.

sphere (1200 $m^2\ g^{-1}$) and PAC (900 $m^2\ g^{-1}$), the CNTs appears most efficient for the removal of $CHCl_3$ from chlorinated drinking water. This could be attributed to the formation of functional groups after acid treatment and the change in wettability of the CNT surface, which made CNTs become more hydrophilic and suitable for the adsorption of relatively low molecular weight and polar THM molecules.

The THMs adsorption data are correlated with the isotherm models of Langmuir (Eq. (4)) and Freundlich (Eq. (5)),

$$q_e = \frac{abC_e}{1 + bC_e} \tag{4}$$

$$q_e = K_f C_e^{1/n} \tag{5}$$

where C_e is the equilibrium concentration of THM molecule ($mg\ l^{-1}$), a the maximum adsorption capacity ($mg\ g^{-1}$), b the Langmuir adsorption constant ($l\ mg^{-1}$) and K_f and n are the Freundlich constants. The constants of the isotherm models at various temperatures were obtained from fitting the isotherm model to the adsorption equilibrium data and are given in Table 2. As can be observed, the adsorption equilibrium data of THMs onto CNTs are better correlated with the Langmuir model. The constants a and K_f, which represent the adsorption capacity of THM molecules, are greater for adsorption of smaller THM molecules and decrease with a rise in temperature, confirming the experimental results of Figs. 7–10. The constant b which reflects the free energy of sorption ($b \propto e^{-\Delta G^\circ/RT}$) presents generally the same trend as the constants a and K_f.

It should be noted that the batch adsorption experiments were carried out in the system of competitive adsorption; the parameters of individual adsorption given in Table 2 correlated each other. That is, if the concentration of one component was changed, the adsorption of other three components will change even if their concentrations were kept at the same value of this study. Furthermore, the adsorption capacity of THM molecules onto CNTs from a pure solution is quite different from a mixed solution. Morawski et al. [16] indicated that the adsorption of $CHCl_3$ onto carbon sphere from a mixed solution is strongly depressed, about 40% of adsorption capacity from a solution of pure $CHCl_3$.

3.5. Thermodynamic analysis

The thermodynamic parameters, free energy change (ΔG°), enthalpy change (ΔH°), and entropy change (ΔS°) for adsorption of THMs onto CNTs were calculated using the following equations [17]:

$$\Delta G^\circ = -RT\ \ln\ K_0 \tag{6}$$

$$\Delta S^\circ = \frac{\Delta H^\circ - \Delta G^\circ}{T} \tag{7}$$

where K_0 is the thermodynamic equilibrium constant. As the THMs concentration in the solution decreases and approaches to 0, values of K_0 are obtained by plotting a straight line of (q_e/C_e) versus q_e based on a least-square analysis and extrapolating q_e to 0. The intercept of vertical axis gives the K_0 value. The ΔH°

Table 2
Constants of Langmuir and Freundlich models of THMs adsorption by CNTs

THM molecules	Temperature (°C)	Langmuir model			Freundlich model		
		a	b	r^2	K_f	$1/n$	r^2
$CHCl_3$	5	3.158	0.00591	0.996	3.116	0.580	0.960
	15	3.054	0.00594	0.999	3.011	0.584	0.951
	25	2.909	0.00506	0.996	2.721	0.595	0.952
	35	2.826	0.00358	0.992	2.383	0.633	0.963
$CHBrCl_2$	5	2.016	0.00182	0.992	1.238	0.574	0.975
	15	1.995	0.00190	0.995	1.215	0.591	0.972
	25	1.994	0.00141	0.996	1.085	0.605	0.977
	35	1.977	0.00092	0.988	0.898	0.635	0.989
$CHBr_2Cl$	5	2.008	0.00175	0.987	1.218	0.636	0.938
	15	1.990	0.00168	0.999	1.169	0.620	0.969
	25	1.976	0.00123	0.994	1.021	0.668	0.974
	35	1.972	0.00089	0.993	0.862	0.727	0.980
$CHBr_3$	5	1.976	0.00125	0.979	1.060	0.612	0.986
	15	1.962	0.00118	0.986	1.025	0.582	0.968
	25	1.960	0.00096	0.988	0.969	1.346	0.997
	35	1.951	0.00078	0.989	0.785	0.795	0.988

Unit: a = mg g^{-1}; b = l mg^{-1}; K_f = (mg g^{-1}) (l mg^{-1})$^{1/n}$; n, r = dimensionless.

is determined from the slope of the regression line after plotting $\ln K_0$ against the reciprocal of absolute temperature, $1/T$. The ΔG° and ΔS° are determined from Eqs. (6) and (7), respectively. Table 3 summaries the values of these thermodynamic parameters. Negative ΔH° indicates the exothermic nature of adsorption process. This is supported by the decrease of THMs adsorption onto CNTs with a rise in temperature, as shown in Figs. 7–10. Negative ΔG° suggests that the adsorption process is spontaneous with a high preference of THM molecules for the CNTs. Positive ΔS°, which reflects the affinity of the CNTs for the THMs and the increase of randomness at the solid/liquid interface during adsorption process, may be due to the release of water molecules produced by molecule exchange between THM molecules and the functional groups attached on the CNT surface [18].

Although the CNTs are efficient adsorbents for the removal of THMs from chlorinated drinking water, the very high unit cost restricts their potential use at the present time [19]. Therefore, developing a new method of manufacturing CNTs to reduce the unit cost of CNTs or testing the reversibility of THMs adsorption onto CNTs to reduce the cost for the replacement of CNTs is needed. Furthermore, before practical use of CNTs in drinking water treatment can be realized, the toxicity of CNTs should be thoroughly investigated. Raw CNTs may possess some degree of toxicity due to the presence of metal catalysts while chemically functionalized CNTs have not demonstrated any toxicity so far. As a result, the practical use of CNTs as adsorbents in water treatment depends upon the continuation of research into the toxicity of CNTs and CNT-related materials [5].

Table 3
Thermodynamic parameters of THMs adsorption by CNTs

THMs	Temperature (°C)	K_0	ΔG° (kJ mol^{-1})	ΔH° (kJ mol^{-1})	ΔS° (J mol^{-1} K^{-1})
$CHCl_3$	5	10.13	−5.355	−1.897	12.439
	15	10.07	−5.535	−1.897	12.632
	25	9.81	−5.661	−1.897	12.631
	35	9.35	−5.724	−1.897	12.425
$CHBrCl_2$	5	8.57	−4.970	−1.989	10.723
	15	8.49	−5.121	−1.989	10.875
	25	8.27	−5.238	−1.989	10.903
	35	7.88	−5.288	−1.989	10.711
$CHBr_2Cl$	5	8.30	−4.894	−2.311	9.291
	15	8.28	−5.062	−2.311	9.522
	25	7.93	−5.133	−2.311	9.470
	35	7.53	−5.171	−2.311	9.286
$CHBr_3$	5	8.19	−4.861	−2.734	7.651
	15	7.75	−4.907	−2.734	7.545
	25	7.73	−5.070	−2.734	7.819
	35	7.30	−5.091	−2.734	7.653

4. Conclusions

The adsorption of THMs from aqueous solution by HNO_3/H_2SO_4 purified MWCNTs at 5, 15, 25 and 35 °C has been investigated to evaluate the kinetics and thermodynamics of adsorption process. As the temperature increased from 5 to 35 °C, the maximum adsorption capacity of $CHCl_3$ calculated by the Langmuir model decreased from 3.158 to 2.826 mg g^{-1}. These values were two to three times more than that of commercially available PAC (1.32 mg g^{-1}) measured at 25 °C in this study, reflecting that CNTs are efficient adsorbents. The kinetics of adsorption process was found to follow the first order rate law. Results of thermodynamic analysis indicated that the adsorption of THMs onto CNTs is exothermic and spontaneous. More studies on the cost-effective analysis of CNTs for the removal of THMs from chlorinated drinking water as well as the toxicity of CNTs and CNT-related materials are needed before practical use of CNTs in drinking water treatment can be realized.

Acknowledgement

Support from the National Science Council, Taiwan, under a contract no. NSC 94-2211-E-005-038 is gratefully acknowledged.

References

[1] C. Chu, C. Lu, C. Lee, C. Tsai, Effects of chlorine level on the growth of biofilm in water pipes, J. Environ. Sci. Health Part A 38 (2003) 1377–1388.
[2] P. Biswas, C. Lu, R.M. Clark, A model for chlorine concentration decay in pipes, Water Res. 27 (11) (1993) 1715–1724.
[3] J.J. Rook, Formation of haloforms during chlorination of natural waters, Water Treat. Exam. 23 (1974) 234–243.
[4] R.J. Bull, L.S. Brinbaum, K.P. Cantor, J.B. Rose, B.E. Butterworth, R. Pegram, J. Tuomisto, Water chlorination: essential process and cancer hazard, Fund. Appl. Toxicol. 28 (1995) 155–166.
[5] S.K. Smart, A.I. Cassady, G.Q. Lu, D.J. Martin, The biocompatibility of carbon nanotubes, Carbon 44 (2006) 1034–1047.
[6] Q.R. Long, R.T. Yang, Carbon nanotubes as superior sorbent for dioxin removal, J. Am. Chem. Soc. 123 (2001) 2058–2059.
[7] Y.H. Li, S. Wang, J. Wei, X. Zhang, C. Xu, Z. Luan, D. Wu, B. Wei, Lead adsorption on carbon nanotubes, Chem. Phys. Lett. 357 (2002) 263–266.
[8] Y. Li, S. Wang, J. Wei, X. Zhang, C. Xu, Z. Luan, D. Wu, Adsorption of fluoride from water by aligned carbon nanotubes, Mater. Res. Bull. 38 (2003) 469–476.
[9] X. Peng, Y. Li, Z. Luan, Z. Di, H. Wang, B. Tian, Z. Jia, Adsorption of 1,2 dichlorobenzene from water to carbon nanotubes, Chem. Phys. Lett. 376 (2003) 154–158.
[10] C. Lu, H. Chiu, Adsorption of zinc (II) from water with purified carbon nanotubes, Chem. Eng. Sci. 61 (4) (2006) 1138–1145.
[11] C. Lu, H. Chiu, C. Liu, Removal of zinc(II) from aqueous solution by purified carbon nanotubes: kinetic and equilibrium studies, Ind. Eng. Chem. Res. 45 (8) (2006) 2850–2855.
[12] Y.H. Li, C. Xu, B. Wei, X. Zhang, M. Zheng, D. Wu, P.M. Ajayan, Self organized ribbons of aligned carbon nanotubes, Chem. Mater. 14 (2002) 483–485.
[13] E. Tütem, R. Apak, C.F. Ünal, Adsorptive removal of chlorophenols from water by bituminous shale, Water Res. 32 (1998) 2315–2324.
[14] W.J. Thomson, Introduction to Transport Phenomena, Prentice Hall PTR, New Jersey, USA, 2000.
[15] G. Atun, T. Sismanoglu, Adsorption of 4, 4′-isopropylidene diphenol and diphenylolpropane 4 4′dioxyacetic acid from aqueous solution on kaolinite, J. Environ. Sci. Health A 31 (1996) 2055–2069.
[16] A.W. Morawski, R. Kalenczuk, M. Inagaki, Adsorption of trihalomethanes (THMs) onto carbon spheres, Desalination 130 (2000) 107–112.
[17] R. Niwas, U. Gupta, A.A. Khan, K.G. Varshney, The adsorption of phosphamidon on the surface of styrene supported zirconium (IV) tungstophosphate: a thermodynamic study, Colloid. Surf. A: Physicochem. Eng. Asp. 164 (2000) 115–119.
[18] Y.H. Li, Z. Di, J. Ding, D. Wu, Z. Luan, Y. Zhu, Adsorption thermodynamic, kinetic and desorption studies of Pb^{2+} on carbon nanotubes, Water Res. 39 (2005) 605–609.
[19] Y.H. Li, J. Ding, Z. Luan, Z. Di, Y. Zhu, C. Xu, D. Wu, B. Wei, Competitive adsorption of Pb^{2+} Cu^{2+} and Cd^{2+} ions from aqueous solutions by multiwalled carbon nanotubes, Carbon 41 (2003) 2787–2792.